USDA
United States Department of Agriculture

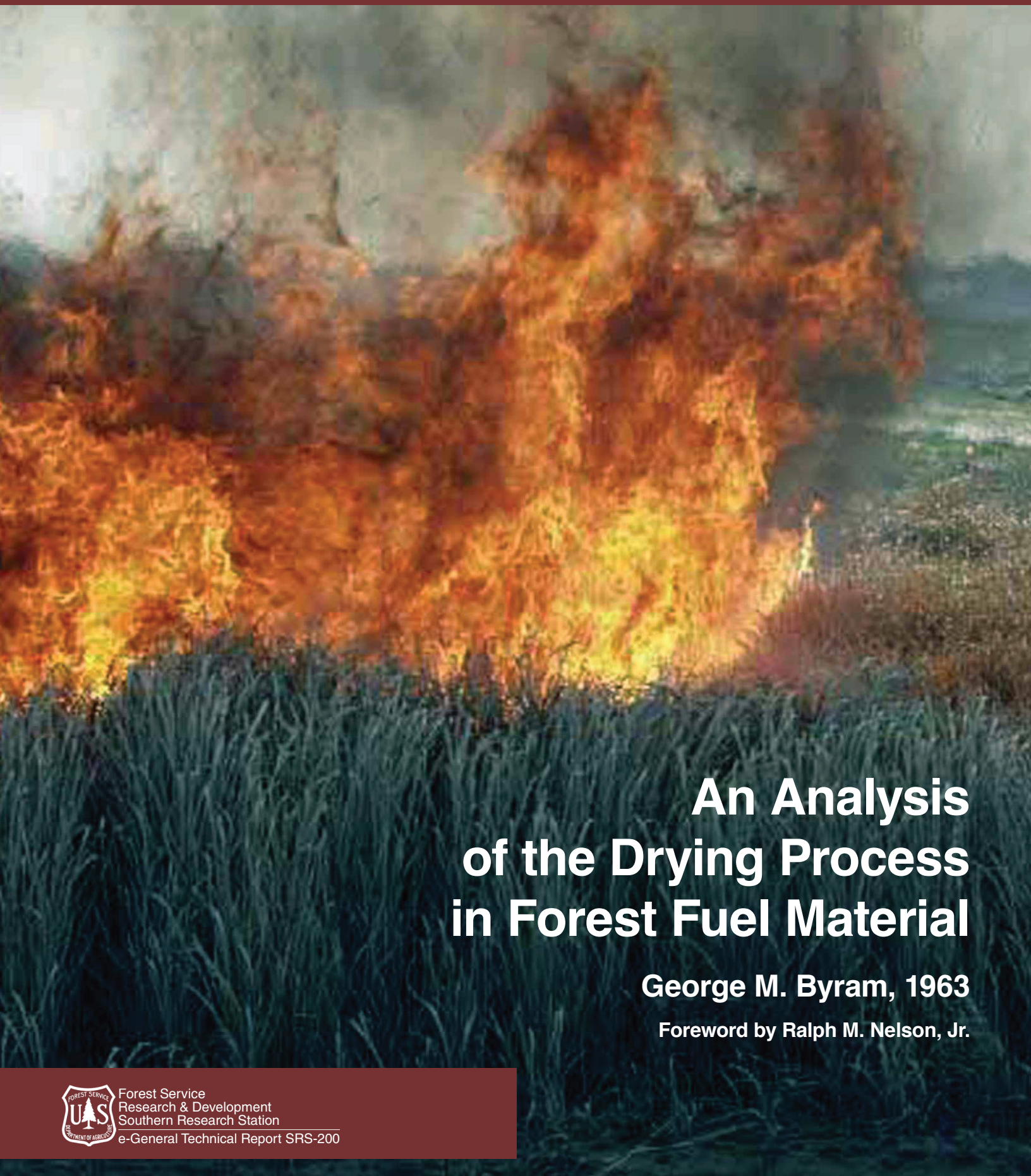

An Analysis of the Drying Process in Forest Fuel Material

George M. Byram, 1963

Foreword by Ralph M. Nelson, Jr.

Forest Service
Research & Development
Southern Research Station
e-General Technical Report SRS-200

The Authors:

George M. Byram, Deceased, Retired as a Forest Fire Research Pioneer in 1968 after working 36 years for the Southeastern Forest Experiment Station, USDA Forest Service; and **Ralph M. Nelson, Jr.**, Retired as a Wood Technologist/ Mechanical Engineer in 2001 after working 14 years for the Missoula Fire Sciences Laboratory and 24 years for the Southern Forest Fire Laboratory, USDA Forest Service.

Cover Photo

Cogongrass wildfire by Charles T. Bryson, USDA Agricultural Research Service, Bugwood.org.

Product Disclaimer

February 2015

Southern Research Station
200 W.T. Weaver Blvd.
Asheville, NC 28804

www.srs.fs.usda.gov

An Analysis of the Drying Process in Forest Fuel Material

George M. Byram, 1963

Foreword by Ralph M. Nelson, Jr.

George M. Byram at his desk ca. 1965

Foreword

Ralph M. Nelson, Jr.

On an autumn afternoon in 1960, I was a wood science graduate student at North Carolina State College in Raleigh checking my experiment when I heard someone speaking my name. After a short visit with me, George Byram was off to the adjacent office to confer with Dr. A.J. Stamm, a wood/physical chemist who was guiding my research. My immediate thought was that they were talking about wood moisture. Three years later, after I had become a full-time staff member at the Southern Forest Fire Laboratory in Macon, GA, I had reason to believe that the earlier Raleigh conversation was about George's analysis of forest fuel drying—the subject of a manuscript I was reviewing for him at the time. Now, some 51 years later, that manuscript is available for readers interested in the technical aspects of fuel drying or in reading Byram's work for historical context. The subject matter will be of special interest to readers looking for details of the mathematical theory of moisture transfer in forest fuels.

HISTORICAL BACKGROUND

George Byram's analysis of the drying of forest fuels has its roots in the history of fire danger rating. The significance of fire danger rating is that fire managers can use it to judge the probability of a fire starting on a given day, how intensely it will burn, and the staffing level required to successfully extinguish the flames. Within the Forest Service, U.S. Department of Agriculture, the concept of fire danger rating originated with Harry Gisborne, who in 1922 was thinking about how there seemed to be differences in fire hazard in different parts of the district in Missoula, MT where he was working. After spending the next 8 years recording observations and writing research papers, Gisborne produced the first fire danger rating system in the form of a meter that rated hazard using data for fuel moisture, wind, and humidity, plus adjustments for human- and lightning-caused risk. Fire managers throughout the United States quickly embraced this primitive method of describing fire danger, adjusting it to fit their local conditions. Over the next 25 years, "new and improved" versions of the meter appeared. However, when managers, scientists, and firefighters from various regions were detailed to a large fire, differences in their meters often caused communication and logistics problems. Consequently, many discussions ensued regarding the status of fire danger rating. One of the considerations at a 1954 fire control conference in Ogden, UT was whether the Forest Service should develop a national system of fire danger rating that would apply uniformly throughout the country (Hardy and Hardy 2007).

In 1958, a committee composed of Forest Service fire research and fire control personnel decided to go forward with development of a new national system. An initial team of researchers began work in 1959, and in 2 years produced a Spread Index ready for nationwide field testing. Because the Index was not applicable in some parts of the country, however, the project was closed. In 1965, a research project established in Seattle, WA surveyed fire control agencies to identify the requirements of a national system and ultimately recommended resuming research on the national system.

By 1968, a National Fire Danger Rating System research unit was established in Fort Collins, CO. Two important project goals were to: (1) develop a nationally uniform system of fire danger rating; and (2) devise a system based on analytical rather than empirical reasoning, with strong emphasis on evaluation of fuel moisture content. After field testing in 1970 and 1971, the unit completed the 1972 version of what is now the National Fire Danger Rating System (NFDRS). In 1975, the Fort Collins project relocated to Missoula, MT and within 3 years produced the improved 1978 NFDRS in use today. In both versions, Byram's fuel drying analysis provided concepts that led to methods of categorizing forest fuels and predicting their moisture content. Updates of the 1978 NFDRS continue to appear as new information and technology become available (Bradshaw and others 1984, Hardy and Hardy 2007).

BYRAM'S ANALYSIS AND THE NATIONAL FIRE DANGER RATING SYSTEM

George Byram joined the Appalachian Forest Experiment Station in 1936 and immediately began studies related to smoke visibility, physics of vision, and fire danger rating. From 1938 to 1943, he conducted creative field experiments that largely clarified the effects of solar radiation, wind speed, temperature, and humidity on the drying of forest fuels and on fuel moisture equilibria. From 1938 to 1965, Byram was primarily a "silent" participant in the development of fire danger rating systems—consulting with colleagues, developing instrumentation pertinent to danger rating, and deriving mathematical expressions for the Buildup and Burning Indexes in the "8" and "8-100" fire danger meters used in the South and East from about 1940 to 1960.

In 1960, Byram formulated a plan of work for current and future staff members of the Southern Forest Fire Laboratory in Macon, GA, the first of three Forest Service fire research centers across the Nation. His problem

analysis identified eight research topics, suggested studies under each topic, and reviewed their status plus the associated research needs. In his discussion of fuel moisture studies, Byram stated:

> *A large part of fire danger rating procedures is equivalent to "keeping books" on the quantity and distribution of fuel moisture. For this reason there will be a continuing need for better fuel moisture studies. Some of the most urgent are detailed studies of drying and moisture replenishment processes designed primarily for the purpose of measuring the relative drying rate for a variety of fuels such as grass, twigs, logs, and duff or litter of varying depth. These studies would require both field and laboratory work.*[1]

Byram followed his own advice by preparing the present manuscript, which consists primarily of mathematical solutions of the well-known diffusion equation for moisture movement in porous materials such as wood and forest fuels. He described the drying of five kinds of fuel particles and of thin layers of litter or duff. Byram also reported the results of laboratory drying tests for comparison with his theoretical work; the experimental results supported the exponential nature of moisture loss with time predicted by the theory. However, the most significant result of Byram's work was that it provided a basis for classifying forest fuels according to their rate of drying—a rate described in terms of the timelag constant (or response time used by some researchers). He showed that under constant ambient conditions, the key variable determining the fuel drying rate is particle thickness or layer depth. Beginning with the 1972 NFDRS and continuing in later versions, system developers used these ideas to partition dead fuels into 1-, 10-, 100-, and 1000-hour classes. Thus, a rapidly drying 1-hour fuel (smaller than 0.64 cm in diameter) represents fuels like grasses or a single weathered needle, whereas a slowly drying 1000-hour fuel would represent logs greater than 8 cm in diameter or a deep layer of duff. This system of fuel classification provides the basis for theoretical calculation of dead fuel moisture content in the ignition, spread, and energy release components of the current NFDRS (Bradshaw and others 1984). Furthermore, the NFDRS method of fuel classification is widely used by fire managers and researchers in activities and studies not directly related to fire danger rating, such as fire behavior and effects experiments, prescribed burning, and numerous modeling efforts.

[1]Byram, G.M. 1960. A problem analysis and proposed research program for the Southern Forest Fire Laboratory. On file with: Fire Research Institute, 943 West Lynwood Drive, San Antonio, Texas 78201. Available electronically from Jason Greenlee at fire_research_institute@hotmail.com.

PUBLISHING DETAILS

Several forest fire researchers have suggested recently that Byram's fuel drying analysis should be published—a proposal they brought forward because of continuing scientific and historical interest in the work. I believe Byram's analysis provides a superb source of information from which fire researchers coming after us can learn the basics of moisture change in forest fuels. It has been cited well over 100 times and continues to appear frequently in papers reporting fuel moisture studies.

The original manuscript was handwritten on yellow legal paper by Byram in the mid-1950s (my dad, a colleague of Byram's, invited his teenaged son to read it). In 1963, he presented an updated version of the analysis to an international conference on humidity and moisture and later submitted it for publication in the proceedings. Reviewers rejected the manuscript, however, claiming the work was not original—the diffusion equation and its solutions had been known for many years. In a sense, they were correct, but they completely missed the significance of the manuscript, which was that Byram's additional work made the equations and their solutions relevant and practical for operational use.

The history of the manuscript reproduced for this General Technical Report (GTR) is uncertain. That Byram edited the submitted manuscript after its rejection seems doubtful. It is more reasonable to assume the manuscript from which this GTR is derived is a photocopy of the one Byram submitted and later distributed to interested parties. This copy has been electronically scanned and included here "as-is," with no textual changes. It was reviewed internally in 1963 but has not undergone today's peer review process. As mentioned earlier, the manuscript was reviewed by conference editors who perhaps could not relate to the stated purpose of the research.

LITERATURE CITED

Hardy, C.C.; Hardy, C.E. 2007. Fire danger rating in the United States of America: an evolution since 1916. International Journal of Wildland Fire. 16: 217-231.

Bradshaw, L.S.; Deeming, J.E.; Burgan, R.E.; Cohen, J.D. 1984. The 1978 National Fire-Danger Rating System: technical documentation. Gen. Tech. Rep. INT-169. Ogden, UT: U.S. Department of Agriculture Forest Service, Intermountain Forest and Range Experiment Station. 44 p.

Ralph M. Nelson, Jr.
Leland, NC
October 2, 2014

An Anal. of the Dry. Proc. in For. Fuels

2429

1-4-67

This report was prepared early in 1963.
Most of the work was done in the period 1960-62

eg m 13

AN ANALYSIS OF THE DRYING PROCESS IN FOREST FUEL MATERIAL

George M. Byram
Southern Forest Fire Laboratory, Southeastern Forest Experiment Station,
U. S. Department of Agriculture, Macon, Georgia

ABSTRACT

It is assumed that the flow of moisture in forest fuels and other woody materials is determined by the gradient of a quantity g which is a function of some property, or properties, of the moisture content. There appears to be no preferred choice for this function, hence moisture transfer equations can be based on a number of equally valid definitions of g. The physical meaning and dimensions of the mass conductivity K_g will depend on the definition of g but the mass diffusivity α is independent of g.

Simplified solutions to the transfer equations are expressed in terms of the ratio t/τ . The timelag τ is a measure of the drying rate. It scales as the second power of the appropriate dimension of the specimen, such as the half thickness, when the Biot number is large but scales as the first power of the characterizing dimension when the Biot number is small. Analytic solutions are not possible when properties are variable but the scaling relationships remain unchanged.

The basic theory of the drying process throws considerable light on the complex interacting effects of air movement, radiation, and evaporation cooling on the drying rates of forest fuel material.

NOMENCLATURE

E, shape factor;

C, moisture concentration in mass per unit volume;

F, $\alpha t/r^2$ (Fourier number);

g, a function of some property, or properties, of m;

g_1, value of g at x = r;

g_e, equilibrium value of g corresponding to H_e;

H, P/P_s (relative vapor pressure);

H_e, relative vapor pressure at infinity;

H_c, relative vapor pressure at x = 0;

h_g, surface transfer coefficient defined by (17);

h_p, surface transfer coefficient for g = P;

K, shape factor;

k_g, mass conductivity defined by (1);

k_p, mass conductivity for g = P;

M, mass,

m, moisture content or mass of water per unit mass of fuel material;

$\bar{m}$, average value of m;

m_o, value of m at t = 0;

$\bar{m}_o$, equivalent value of m_o defined by (30);

m_1, value of m at x = r;

m_e, equilibrium moisture content corresponding to H_e;

N_M, $\lambda_M r$;

P, vapor pressure at any given point within a fuel specimen;

P_o, value of P at t = 0;

P_1, value of P at x = r;

P_e, vapor pressure at infinity;

P_c, value of P at x = 0;

P_s, saturation vapor pressure;

R, drying rate ratio defined in (37);

r, radius or half thickness of specimen;

S_1, S_2, sums of series in (34) and (35);

T, temperature;

t, time;

x, y z, space coordinates;

Greek symbols

α, mass diffusivity;

β, $\left(\frac{\partial m}{\partial H}\right)_T$;

λ_M, roots of eigenfunction equations;

ρ, density;

τ, $r^2/N_1^2 \cdot \alpha$ (timelag).

INTRODUCTION

One of the most important factors influencing the intensity of forest fires is the amount of water in the burning fuel. Hence, any procedure for measuring or estimating the flammability of such fuels must give considerable weight to their moisture content and its distribution. Forest fuels are a heterogeneous mixture of woody materials in which the individual components may vary greatly in size, shape, and arrangement. Intermingled with the nonliving fuel to a greater or lesser extent are green or living plants. They constitute another component of the total forest fuel material.

This paper is concerned primarily with the theoretical aspects of the loss of moisture in the nonliving fuels--especially in the moisture content range below the fiber saturation point, where the flammability of forest fuels increases rapidly with decreasing moisture content. The main objective is to obtain a mathematical description of the drying process which can be readily compared with experimental data.

Among the numerous papers in the literature on drying, there are a considerable number which apply to the drying of wood or materials similar to wood. A few examples are the papers by Tuttle (11), Sherwood (8), Hougen, McCauley, and Marshall (6), Stamm (10), and Van Arsdel (12). An extensive summary account of the drying of solids is given by Marshall and Friedman (7).

In formulating theories of the drying process, investigators have used different assumptions as to the nature of the gradient responsible for the flow of moisture in the drying material. One assumption is that a moisture gradient determines the flow, and some problems in diffusion are approached from this viewpoint. Another assumption is that the moisture flow is determined by the vapor pressure gradient. Van Arsdel (12) points out that, in the absence of a temperature gradient, the choice between these two assumptions is only a matter of convenience. However, other choices of gradient are equally valid and among the various possible gradients none can be designated as the preferred choice. This somewhat confusing point can be clarified considerably by postulating that the moisture flow is determined by the gradient of a quantity g which is a function of some property, or combination of properties, of the moisture in the drying material. On the basis of this assumption one can then write the equation

$$\frac{dM}{dt} = -k_g A \frac{dg}{dx} \qquad (1)$$

where $\frac{dM}{dt}$ is the rate of mass flow of moisture through an area A perpendicular to the direction of flow, and $\frac{dg}{dz}$ is the gradient of g in the direction of flow. The quantity k_g is defined by this equation. It may be designated as the moisture or mass conductivity and corresponds to the thermal conductivity in heat transfer. Although k_g is numerically equal to the rate of moisture flow per unit of cross section area per unit of gradient of g, its physical meaning and dimensions will depend on the definition of g.

MOISTURE TRANSFER EQUATIONS

The fundamental equation of moisture flow based on equation (1) can be written as

$$\frac{\partial\left(k_g \frac{\partial g}{\partial x}\right)}{\partial x} + \frac{\partial\left(k_g \frac{\partial g}{\partial y}\right)}{\partial y} + \frac{\partial\left(k_g \frac{\partial g}{\partial z}\right)}{\partial z} = \frac{\partial C}{\partial t} \qquad (2)$$

where C is the mass of water per unit volume, or the moisture concentration in the drying material. This equation may be regarded as a general form of Fick's diffusion equation. The next step is to express g in terms of some property, or properties, of the moisture content. One choice is the relationship g = P, which is equivalent to the assumption that the moisture flow is determined by the vapor pressure gradient. If g = P, then equation (2) can be written as

$$\frac{\partial\left(k_p \frac{\partial P}{\partial x}\right)}{\partial x} + \frac{\partial\left(k_p \frac{\partial P}{\partial y}\right)}{\partial y} + \frac{\partial\left(k_p \frac{\partial P}{\partial z}\right)}{\partial z} = \frac{\partial C}{\partial t} \qquad (3)$$

in which k_g has been designated as k_p when $g = P$.

At this point it is desirable to introduce the dimensionless quantity β, which is defined by the equation

$$\beta = \left(\frac{\partial m}{\partial H}\right)_T$$

where m is moisture content and is defined as the mass of water per unit mass of fuel in the fuel-water mixture. The relative vapor pressure H is given by the relationship[1/] $H = P/P_s$ where P_s is the

---

1/ H has values between 0 and 1 and m has values between 0 and ∞. For convenience they are usually multiplied by 100 and expressed in percent, in which case H is known as relative humidity and m as percent moisture.

---

saturation vapor pressure at temperature T. The defining equation for β shows that this quantity is the slope of a vapor pressure isotherm in which m is expressed as a function of H.

The moisture concentration C may be expressed as

$$C = \rho m \qquad (4)$$

where ρ is the density[2/] of the fuel component of the fuel-water

---

2/ The density ρ is based on the bone dry fuel weight and the volume at moisture content m.

---

ixture. If at any point in the drying substance the temperature T and density ρ are not changing with time, equation (4) can be differentiated and expressed successively by the series of equations

$$\frac{\partial c}{\partial t} = \rho \frac{\partial m}{\partial t} = \rho \left(\frac{\partial m}{\partial P}\right)_T \frac{\partial P}{\partial t} = \frac{\rho}{\rho_s}\left(\frac{\partial m}{\partial H}\right)_T \frac{\partial P}{\partial t} = \frac{\rho \beta}{\rho_s} \frac{\partial P}{\partial t} \tag{5}$$

Owing to shrinkage, the density ρ at a given point will decrease with time as the drying progresses but the change is small and can be neglected. Equation (3) can now be written as

$$\frac{\partial\left(k_p \frac{\partial P}{\partial x}\right)}{\partial x} + \frac{\partial\left(k_p \frac{\partial P}{\partial y}\right)}{\partial y} + \frac{\partial\left(k_p \frac{\partial P}{\partial z}\right)}{\partial z} = \frac{\rho \beta}{\rho_s} \frac{\partial P}{\partial t} \tag{6}$$

This equation describes the drying process even though k_p and β are variable. If k_p is constant, equation (6) takes the simplified form

$$\frac{\partial^2 P}{\partial x^2} + \frac{\partial^2 P}{\partial y^2} + \frac{\partial^2 P}{\partial z^2} = \frac{1}{\alpha} \frac{\partial P}{\partial t} \tag{7}$$

where α may be defined as the mass diffusivity and is given by the relationship

$$\alpha = \frac{k_p P_s}{\rho \beta} \tag{8}$$

One of the most effective choices for the function g is $g = m P_s$. If P_s is not changing with time, then

$$\frac{\partial g}{\partial t} = P_s \frac{\partial m}{\partial t} \tag{9}$$

Combining equation (9) with the relationship $\frac{\partial C}{\partial t} = \rho \frac{\partial m}{\partial t}$ and substituting the result for $\frac{\partial C}{\partial t}$ in the right member of equation (2) gives when written in terms of m

$$\frac{\partial \left(k_g \frac{\partial m}{\partial x}\right)}{\partial x} + \frac{\partial \left(k_g \frac{\partial m}{\partial y}\right)}{\partial y} + \frac{\partial \left(k_g \frac{\partial m}{\partial z}\right)}{\partial z} = \frac{\rho}{P_s} \frac{\partial m}{\partial t} \tag{10}$$

If k_g is constant and if there are no temperature gradients in the drying material, then equation (10) becomes

$$\frac{\partial^2 m}{\partial x^2} + \frac{\partial^2 m}{\partial y^2} + \frac{\partial^2 m}{\partial z^2} = \frac{\rho}{k_g P_s} \frac{\partial m}{\partial t} = \frac{1}{\alpha} \frac{\partial m}{\partial t} \tag{11}$$

where

$$\alpha = \frac{k_g \rho_s}{\rho} \tag{12}$$

Pairs of equations, analogous to equations (6) and (7), or (10) and (11), based on other choices of g will not be given. However, the relations between the k's and the α's for isothermal conditions are summarized for five different functions for g in table 1. All of the α's are identical and have the dimensions L^2t^{-1}. Each of the k's is different, although for $g = P$ and $g = mP_s$ the two corresponding k's each have the dimensions of time. For simplicity the k for $g = mP_s$ is designated as k_g and all other k's are expressed in terms of k_g. Table 1 illustrates the arbitrary nature of the gradient which is assumed to determine the flow of moisture. The procedure for finding the relationships between the k's can be illustrated by determining the relationship between k_g and k_p. By letting g take the forms of $g = mP_s$ and $g = P$, it follows from equation (1) that for isothermal conditions

$$k_g \frac{\partial g}{\partial x} = k_g \rho_s \frac{\partial m}{\partial x} = k_p \frac{\partial P}{\partial x}$$

Also for isothermal conditions

$$k_g \rho_s \frac{\partial m}{\partial x} = k_g \rho_s \left(\frac{\partial m}{\partial P}\right)_T \frac{\partial P}{\partial x} = k_g \beta \frac{\partial P}{\partial x}$$

Table 1.--A summary of the k's and α's with their physical dimensions corresponding to five different choices for the function g

g	k	Dimensions of k	α (Dimensions are L^2t^{-1})
mP_s	k_g	t	$\alpha_g = \frac{k_g P_s}{\rho}$
P	$k_p = \beta k_g$	t	$\alpha_p = \frac{k_p P_s}{\rho\beta} = \frac{k_g P_s}{\rho}$
m	$k_m = P_s k_g$	$ML^{-1}t^{-1}$	$\alpha_m = \frac{k_m}{\rho} = \frac{k_g P_s}{\rho}$
C	$k_c = \frac{P_s k_g}{\rho}$	L^2t^{-1}	$\alpha_c = k_c = \frac{k_g P_s}{\rho}$
CP_s	$k_{cp} = \frac{k_g}{\rho}$	$M^{-1}L^3t$	$\alpha_{cp} = P_s k_c = \frac{k_g P_s}{\rho}$

Therefore

$$k_p = \beta k_g$$

For a substance for which the vapor pressure isotherms are linear (Henry's law) β is constant. In this case k_p would be directly proportional to k_g. If either k_p or k_g were constant, the other would also be constant. However, for most substances β is variable, so ordinarily both k's could not be constant. The vapor pressure isotherms shown in figure 1 for temperatures of 72°F. and 90°F. are those which Spalt (9) obtained for desorption conditions for basswood. Figure 2 shows β plotted as a function of m for temperatures of 72°F. and 90°F. Ordinates of these curves were obtained by measuring the slopes of the curves in figure 1. Either curve shows that β can be taken as approximately constant for values of m between 0.05 and 0.12 but increases rapidly as m approaches the fiber saturation point.

Figure 1.--Vapor pressure isotherms for temperatures of 72°F. and 90°F. show the moisture content m plotted as a function of the relative vapor pressure H. These curves are those which Spalt (9) obtained for basswood for desorption conditions.

Figure 2.--The parameter β is shown as a function of the moisture content m for temperatures of 72°F. and 90°F. The ordinates of these curves are equal to the slopes of the curves in figure 1.

SOLUTIONS TO THE MOISTURE TRANSFER EQUATIONS

When the fuel properties are variable, solutions to the moisture transfer equations have to be obtained by graphical or numerical methods. However, much can be learned about the general drying process from analytic solutions based on the assumption that the properties of the drying material, on certain combinations of properties, are constant. Such solutions are also useful approximations even when the properties are not constant.

A wide variety of solutions is available in the literature of heat and mass transfer. An important example is the solution for the infinite cylinder, which is significant for isolated individual materials like logs, dead limbs, and certain types of cured grass stems. Solutions for the infinite slab would apply to individual leaves, thin grass blades, isolated layers of bark and wood, and to a layer of duff over a rocky surface impervious to the passage of moisture. Deep layers of duff and organic soils can best be treated as semi-infinite solids. For all of these cases the moisture transfer equations can be written in one dimensional form.

Solutions based on equation (11) can be expressed directly in terms of the moisture content, so this equation is ordinarily the most suitable to use. Consider an infinite cylinder of woody material of radius r with a uniform initial moisture content of m_o which is

drying in an atmosphere of constant temperature and constant relative vapor pressure for which the equilibrium moisture content is m_e. If m is the moisture content at any radial distance x from the cylinder axis at time t, equation (11) in cylindrical coordinates becomes

$$\frac{1}{x}\frac{\partial\left(x\frac{\partial m}{\partial x}\right)}{\partial x} = \frac{1}{\alpha}\frac{\partial m}{\partial t} \qquad (13)$$

The initial conditions are

$$m - m_e = m_o - m_e \qquad \text{when } t = 0$$

The boundary conditions are

$$\frac{\partial(m-m_e)}{\partial x} = 0 \qquad \text{at } x = 0$$

and

$$-k_g\frac{\partial(m-m_e)}{\partial x} = h_g(m-m_e) \qquad \text{at } x = r$$

where h_g is the surface transfer coefficient.

The solution to equation (13) is[3/]

$$\frac{m-m_e}{m_o-m_e} = 2\sum_{m=1}^{\infty} \frac{1}{N_m} \frac{J_1(N_m)}{J_0^2(N_m)+J_1^2(N_m)} e^{-N_m^2(at/r^2)} J_0\left(N_m \frac{x}{r}\right) \quad (14)$$

3/ Details of solutions for objects of various shapes are given in works on diffusion and heat transfer such as those of Crank (3), Giedt (5), Eckert and Drake (4), and Carslaw and Jaeger (2). As in heat transfer theory, the dimensionless groups at/r^2 and $h_g r/k_g$ may be designated as the Fourier number and Biot number, respectively.

---

where $N_n = \lambda_n r$ and λ_n represents roots of the eigenfunction equation

$$\lambda_m r J_1(\lambda_m r)/J_0(\lambda_m r) = h_g r/k_g \quad (15)$$

J_0 is a Bessel function of the first kind and zero order and J_1 is a Bessel function of the first kind and first order.

In experimental work, the average moisture content is much easier to determine than the moisture content at a given point within a specimen, so it is desirable to have solutions to the equations

expressed in terms of the average moisture. If $\bar{m}$ is the average moisture content throughout the cylinder then

$$\bar{m} - m_e = (m - m_e)_{av} = \frac{2}{r^2}\int_0^r (m - m_e)\, r\, dr$$

Substituting in this equation the value of $m - m_e$ given by equation (14) and integrating gives

$$\frac{\bar{m} - m_e}{m_0 - m_e} = 4\sum_{n=1}^{\infty} \frac{1}{N_n^2} \frac{J_1^2(N_n)}{J_0^2(N_n) + J_1^2(N_n)} e^{-N_n^2 (\alpha t / r^2)} \qquad (16)$$

The value of N_n in equations (14) and (16) will depend on the ratio $h_g r/k_g$ in equation (15). The surface transfer coefficient h_g is defined by the general equation

$$\frac{dM}{dt} = -h_g A (g_1 - g_e) \qquad (17)$$

where $\frac{dM}{dt}$ is the rate of mass flow of moisture through a surface of area A, g_1 is the value of g at the surface of the specimen, and g_e is the equilibrium value of g for an environmental relative vapor pressure H_e. For $g = mP_s$ equation (17) becomes

$$\frac{dM}{dt} = -h_g A P_s (m_1 - m_e) \qquad (18)$$

Equation (16) takes on a much simpler form if the resistance to the flow of moisture through the surface is negligible compared to the internal resistance to moisture flow. In this case the Biot number $h_g r/k_g$ is very large. In equations (14) and (16), $J_o(N_n) \longrightarrow 0$ as $h_g r/k_g \longrightarrow \infty$. Equation (16) then takes the limiting form

$$\frac{\bar{m}-m_e}{m_o-m_e} = 4\sum_{m=1}^{\infty} \frac{1}{N_m^2} e^{-N_m^2(\alpha t/r^2)}$$

$$= 4\left[\frac{1}{N_1^2} e^{-N_1^2(\alpha t/r^2)} + \frac{1}{N_2^2} e^{-N_2^2(\alpha t/r^2)} + \cdots\cdots\right] \qquad (19)$$

in which N_1, N_2, ... N_n are the successive zeros of $J_o(N_n)$. Equation (19) is represented by curve A in figure 3, in which $\frac{\bar{m}-m_e}{m_o-m_e}$ is shown on a semi-log chart as a function of the Fourier number $\alpha t/r^2$.

Figure 3.--Theoretical drying curves for specimens with six different geometric forms: A, cylinder; B, infinite plane slab; C, infinite square rod; D, cube; E, sphere; F, semi-infinite solid. The ratio $(\bar{m}-m_e)/(m_o-m_e)$ is plotted as a function of the Fourier number $\alpha t/r^2$.

$\alpha\alpha = 2.404\varepsilon$

With the exception of the brief initial period when the moisture distribution is becoming established, this curve is linear. This is a result of the rapid convergence of the series in equation (19). For values of $\alpha t/r^2$ greater than 0.10, only the first term need be retained, and equation (19) can be written approximately as

$$\frac{\bar{m}-m_e}{m_0-m_e} = \frac{H}{N_1^2} e^{-N_1^2(\alpha t/r^2)} \qquad \text{cylinder} \tag{20}$$

For an infinite plane slab, equation (11) reduces to

$$\frac{\partial^2 m}{\partial x^2} = \frac{1}{\alpha}\frac{\partial m}{\partial t}$$

in which x is measured from the slab center. The initial conditions and boundary conditions are the same as for equation (13). For a slab of thickness 2r, the solution is[3]

$$\frac{m-m_e}{m_0-m_e} = 2\sum_{n=1}^{\infty} \frac{\sin N_n}{N_n + \sin N_n \cos N_n} e^{-N_n^2(\alpha t/r^2)} \cos\left(N_n \frac{x}{r}\right) \tag{21}$$

where $N_n = \lambda_n r$ and λ_n represents the roots given by the equation

$$\cot \lambda_n r = \cot N_n = \frac{h_g \lambda_n}{h_g} = \frac{N_n}{h_g r/k_g} \tag{22}$$

When expressed in terms of $\bar{m} - m_e$, the solution for the slab is

$$\frac{\bar{m}-m_e}{m_o-m_e} = 2\sum_{n=1}^{\infty} \frac{\sin^2 N_n}{N_n(N_n+\sin N_n \cos N_n)} e^{-N_n^2(\alpha t/r^2)} \tag{23}$$

When $h_g r/k_g$ is very large, equation (23) also takes a simpler form. As $h_g r/k_g \longrightarrow \infty$, $\cot N_n \longrightarrow 0$, and $N_n \longrightarrow (2n-1)\pi/2$. Equation (23) then becomes

$$\frac{\bar{m}-m_e}{m_o-m_e} = 2\sum_{n=1}^{\infty} \frac{1}{N_n^2} e^{-N_n^2(\alpha t/r^2)}$$

$$= \frac{8}{\pi^2}\left[e^{-\left(\frac{\pi}{2}\right)^2(\alpha t/r^2)} + \frac{1}{3^2} e^{-\left(\frac{3\pi}{2}\right)^2(\alpha t/r^2)} + \frac{1}{5^2} e^{-\left(\frac{5\pi}{2}\right)^2(\alpha t/r^2)} + \cdots \right] \tag{24}$$

which is represented by curve B in figure 3. As in the cylindrical case, the series in equation (24) also converges very rapidly and the straight line portion of curve B represents only the first term. Equation (24) then reduces to

$$\frac{\bar{m}-m_e}{m_o-m_e} = \frac{8}{\pi^2} e^{-\left(\frac{\pi}{2}\right)^2(\alpha t/r^2)} \tag{25}$$

By the use of the product method[3], solutions in one dimension can be applied to objects of numerous shapes. An example is the infinitely long square rod. In this case it can be shown that the solution is the square of the right member of equation (23) or equation (24) for the infinite plane slab. If only one term in the resulting series is retained, the equation analogous to equation (25) is

$$\frac{\overline{m} - m_e}{m_o - m_e} = \left(\frac{8}{\pi^2}\right)^2 e^{-2\left(\frac{\pi}{2}\right)^2 (\alpha t / r^2)} \tag{26}$$

where 2r is the diameter of the rod. Similarly, the equation for a cube of diameter 2r is

$$\frac{\overline{m} - m_e}{m_o - m_e} = \left(\frac{8}{\pi^2}\right)^3 e^{-3\left(\frac{\pi}{2}\right)^2 (\alpha t / r^2)} \tag{27}$$

In figure 3, equations (26) and (27) are represented by the straight line portions of curves C and D, respectively.

Curve E in figure 3 is the drying curve for a sphere of radius r. The straight line portion of the curve represents the equation

$$\frac{\overline{m} - m_e}{m_o - m_e} = \frac{6}{\pi^2} e^{-\pi^2 (\alpha t / r^2)} \tag{28}$$

Equation (20) as well as equations (25) through (28) can all be expressed by the single equation

$$\frac{\bar{m} - m_e}{m_o - m_e} = K e^{-t/\tau} \tag{29}$$

in which τ is a quantity which has the dimensions of time. It represents the combination of factors which comprise the coefficients of t in the different drying equations. Physically τ is equal to the time required for the value of $\bar{m} - m_e$ at some arbitrarily chosen point on the linear portion of any of the curves in figure 3 to drop to 1/e of the value at the beginning of the interval. It is defined as the timelag and is a very useful parameter for comparing the drying characteristics of different forest fuel materials. The dimensionless constant K depends on the shape of the drying specimen. Geometrically it represents the intersection of the extension of the straight line portion of the curves in figure 3 with the t = 0 ordinate. For example, in curve B, the value of K is $8/\pi^2$. Equation (29) can also be written as

$$\frac{\bar{m} - m_e}{m_o - m_e} = e^{-t/\tau} \tag{30}$$

in which $\bar{m}_o - m_e = K(m_o - m_e)$ and represents an adjusted or equivalent value of $\bar{m} - m_e$ for $t = 0$.

An additional case of considerable practical significance is the semi-infinite solid which is approximated by a deep layer of duff or organic soil. Throughout a surface layer in which the depth r is small compared to the total depth, $\bar{m} - m_e$ can be expressed as an integral of the error function. If constant properties are assumed and if h_g is very large, the equation for $\bar{m} - m_e$ can be written as

$$\frac{\bar{m} - m_e}{m_o - m_e} = \frac{2}{r\sqrt{\pi}} \int_0^r \int_0^{x/2\sqrt{\alpha t}} e^{-u^2} du\, dx$$

Placing e^{-u^2} in a power series form and integrating term by term gives

$$\frac{\bar{m} - m_e}{m_o - m_e} = \frac{F^{-1/2}}{2\sqrt{\pi}} \left[1 - \frac{(4F)^{-1}}{2 \cdot 3 \cdot 1!} + \frac{(4F)^{-2}}{3 \cdot 5 \cdot 2!} - \frac{(4F)^{-3}}{4 \cdot 7 \cdot 3!} + \cdots \right] \qquad (31)$$

where $F = \alpha t / r^2$. This equation is represented by curve F in figure 3. In this case the logarithm of $\bar{m} - m_e$ does not become linear with increasing values of $\alpha t / r^2$ as in all of the other cases but decreases at a diminishing rate. This is caused by moisture traveling upward from deeper layers in the semi-infinite material. The thickness of the surface layer is taken as r rather than 2r because, unlike the slab, it can lose moisture from only one side.

DRYING RATES

The Effect of Temperature and Relative Vapor Pressure

To examine the effect of temperature and relative vapor pressure on the drying rate, it is somewhat simpler to work with vapor pressure gradients rather than with gradients of mP_s. Taking the infinite slab of thickness 2r as an example, the solution of equation (7) in one dimension is

$$\frac{P-P_e}{P_o-P_e}=2\sum_{n=1}^{\infty}\frac{\sin N_n}{N_n+\sin N_n\cos N_n}\,e^{-N_n^2(\alpha t/r^2)}\cos\left(N_n\frac{x}{r}\right) \qquad (32)$$

where P is the vapor pressure in the drying material at a distance x from the slab center, P_e the vapor pressure at infinity, and P_o the vapor pressure within the specimen at time t = 0 when the moisture content m was uniform.

The form of the right members of equations (21) and (32) are identical but N_n is not the same in both cases. In equation (21) N_n is a function of $h_g r/k_g$ and in equation (32) it is a function of $h_p r/k_p$. The surface transfer coefficient h_p is defined by equation (17) with P_i replacing g_i, P_e replacing g_e, and h_p replacing h_g.

The outward rate of mass flow of moisture across the surface is

$$\frac{dM}{dt}=-h_p\left(\frac{\partial P}{\partial x}\right)_{x=r}. \qquad (33)$$

where $\frac{dM}{dt}$ now represents the mass flow per unit of surface area and $(\partial P/\partial x)_{x=r}$ is the vapor pressure gradient at the surface. Differentiating equation (32) and letting x = r gives

$$\left(\frac{\partial P}{\partial x}\right)_{x=r} = (P_o - P_e)\frac{2}{r}\sum_{m=1}^{\infty} \frac{N_m \sin N_m}{N_m + \sin N_m \cos N_m} e^{-N_m^2 (\alpha t/r^2)} \tag{34}$$

When x = 0, equation (32) becomes

$$\frac{P_c - P_e}{P_o - P_e} = 2\sum_{m=1}^{\infty} \frac{\sin N_m}{N_m + \sin N_m \cos N_m} e^{-N_m^2 (\alpha t/r^2)} \tag{35}$$

where P_c is the vapor pressure at the slab center. Combining equations (33), (34), and (35) gives for the outward moisture flux

$$\frac{dM}{dt} = -\frac{k_p}{r}(P_c - P_e)\, S_1/S_2 \tag{36}$$

where S_1 is the sum of the series in equation (34) and S_2 the sum of the series in equation (35). A drying rate ratio R may be defined as

$$R = \frac{dM}{dt} \Big/ \left(\frac{dM}{dt}\right)'$$

in which $\frac{dM}{dt}$ is the outward flux of moisture for vapor pressures of P_c and P_e and $\left(\frac{dM}{dt}\right)'$ the flux for vapor pressure P_c' and P_e'. The drying rate ratio makes it possible to compare the drying rate of two identical specimens in environments with different temperatures and different relative vapor pressures.

Using equation (36), the drying rate ratio can be written as

$$R = \frac{P_c - P_e}{P_c' - P_e'} \frac{S_1}{S_2} \frac{S_2'}{S_1'}$$

If $\alpha t/r^2$ is chosen so that this group is the same for both specimens, then $S_1 = S_1'$ and $S_2 = S_2'$. R can then be written in the alternate forms

$$R = \frac{P_c - P_e}{P_c' - P_e'} = \frac{H_c - H_e}{H_c' - H_e'} \frac{P_s}{P_s'} \tag{37}$$

where P_s and P_s' are the saturation vapor pressures for temperatures T and T' in the two environments, H_e and H_e' are the corresponding relative vapor pressures in the environments, and H_c and H_c' are the relative vapor pressures at the slab centers.

If the moisture content at the center of the two slabs is high, then P_c and P_c' are nearly equal to the saturation vapor pressures P_s and P_s', respectively. Equation (37) can then be

written in the approximate form

$$R = \frac{(1 - H_e)\, P_s}{(1 - H_e')\, P_s'} \tag{38}$$

which can be used for estimating R when the central moisture content m_c is 0.20 or more and if H_e and H_e' are 0.40 or less. For smaller values of m_c and higher values of H_e and H_e', equation (37) should be used. The values of H_c and H_c' corresponding to m_c and m_c' can be read from the vapor pressure isotherms. The central moisture can be determined from the average moisture which for the slab is given by the equation

$$m_c - m_e = \frac{\pi}{2}\left(\bar{m} - m_e\right)$$

provided that $h_g r/k_g$ is large and the drying periods are long enough for the moisture distribution to become established. This distribution begins to approach its final form at relatively small values of $\alpha t/r^2$ as shown in figure 4. This diagram is a plot of equation

Figure 4.--The theoretical distribution of moisture across a plane slab at time $t = \tau/2$.

(21) for $t = \tau/2$, or $\alpha t/r^2 = 2/\pi^2$, and $h_g r/k_g = \infty$ and represents the theoretical distribution of $\frac{m - m_e}{m_o - m_e}$ across the slab.

It can be shown that equations (37) and (38) apply to specimens of other shapes such as cubes, spheres, and rods. However, for a finite surface layer of a semi-infinite material, the drying rate ratio becomes

$$R = \left(\frac{H_c - H_e}{H_c' - H_e'}\right)\left(\frac{P_s}{P_s'}\right)^{1/2}$$

For two identical specimens drying in environments for which the specimen temperatures are T and T' the ratio of their timelags will be

$$\tau/\tau' = P_s'/P_s$$

This ratio should not be confused with the drying rate ratio R in equation (37) although both are a measure of relative drying rates. R represents the ratio of the rates when either rate is expressed in units of mass of water per unit time; τ/τ' represents the ratio of the reciprocal of the rates of change of $\log(\bar{m} - m_e)$ which, with the exception of the semi-infinite case, are constant when the drying curves (figure 3) become linear. The magnitude of τ/τ' does not depend on the relative vapor pressure.

The Effect of Fuel Size or Thickness of Fuel Layer on the Drying Rate

Equations such as (14) and (21) express $m - m_e$ as a function of three dimensionless groups N_n, $\alpha t/r^2$, and x/r. In equations

for $\bar{m} - m_e$, such as (16) and (23), only the groups N_n and $\alpha t/r^2$ appear because $x/r = 1$. It is not readily apparent from any of these equations just how the time required for $m - m_e$, or $\bar{m} - m_e$, to decrease to some given fraction of $m_o - m_e$ depends on the dimension r because the values of N_n also depend on r. However, N_1 , N_2 , ... N_n approach constant values in the limiting cases for which $h_g r/k_g \longrightarrow \infty$ and $h_g r/k_g \longrightarrow 0$. Examples of the first case are represented by equations (19) and (24), in which only the group $\alpha t/r^2$ appears as a variable in the right member of the equations. In this case it is obvious that the time required for $\bar{m} - m_e$ to drop to a given fraction of $m_o - m_e$ varies as r^2 . The same relationship holds for specimens of other shapes, including a finite surface layer of thickness r which is part of a semi-infinite material. The second power relationship also applies to $m - m_e$ at any given value of x/r in equations (14) and (21) as $h_g r/k_g \longrightarrow \infty$ except at the surface, where $x/r = 1$ and $m - m_e = 0$. The same results are obtained with equations based on the other functions for g given in table 1.

The form which the equations for $\bar{m} - m_e$ takes when $h_g r/k_g \longrightarrow 0$ can be most easily determined from equation (23). $N_m \longrightarrow (m-1)\pi$ as $h_g r/k_g \longrightarrow 0$ and all terms in the series vanish except the first, for

which n = 1. This term is the product of the term $e^{-N_1^2(\alpha t/r^2)}$ and the indeterminate fraction

$$\frac{\sin^2 N_1}{N_1(N_1 + \sin N_1 \cos N_1)}$$

which approaches 1/2 as $N_1 \longrightarrow 0$. From equation (22)

$$N_1 \tan N_1 = h_g r/k_g$$

Since $\tan N_1 \longrightarrow N_1$ as $N_1 \longrightarrow 0$, it follows that $N_1^2 = h_g r/k_g$ for very small values of $h_g r/k_g$. In this case equation (23) thus takes the limiting form

$$\frac{\bar{m} - m_e}{m_o - m_e} = e^{-(h_g r/k_g)(\alpha t/r^2)} = e^{-h_g \rho_s t/\rho r} \qquad (39)$$

The time required for $\bar{m} - m_e$ to reach a given fraction of $m_o - m_e$ thus varies as r when $h_g r/k_g$ is very small. Equation (21) also approaches equation (39) as $h_g r/k_g \longrightarrow 0$. This means $m = \bar{m}$ for all values of r and moisture gradients in the drying material vanish in this limiting case.

From its definition the timelag τ for specimens of different shapes can be expressed in the forms

$$\tau = \frac{r^2}{N_1^2 \alpha} = \frac{r^2 \rho}{N_1^2 k_g \rho_s}$$

For large values of $h_g r/k_g$, N_1 is a constant whose value depends on the specimen shape. For very small values of $h_g r/k_g$, N_1 becomes

$$N_1^2 = \frac{1}{B} \frac{h_g r}{k_g}$$

where B is a dimensionless constant which also depends on the specimen shape. When $h_g r/k_g$ is very small, the equation for τ then becomes

$$\tau = \frac{B r \rho}{h_g P_3} \tag{40}$$

Thus there is a second power relationship between τ and r when the Biot number is large, and a first power relationship when the Biot number is small.

The derivation of the relationships between τ and r has been based on the analytic solutions to the moisture transfer equations. In turn, such solutions were possible only because of certain simplifying assumptions including that of constant k_g. The question then arises as to whether the relationships between τ and r hold when k_g is variable. It can be shown that they do by means of a similarity argument.

In equation (10), let x, y, z, and t be replaced with dimensionless X, Y, Z, and t' such that

$$X = x/r, \quad Y = y/r, \quad Z = z/r, \quad \text{and} \quad t' = t/\tau$$

where r is some appropriate dimension of the specimen such as its radius or half thickness and τ is the timelag for the specimen with the dimension r. Also let k_g be variable and given by the equation

$$k_g = k_g' f(m)$$

where f(m) is a dimensionless function of m and k_g' is constant and represents the value of k_g for some given value of m. Equation (10) can then be written as

$$\frac{\partial\left(f\frac{\partial m}{\partial X}\right)}{\partial X} + \frac{\partial\left(f\frac{\partial m}{\partial Y}\right)}{\partial Y} + \frac{\partial\left(f\frac{\partial m}{\partial Z}\right)}{\partial Z} = \frac{\rho r^2}{\rho_s k_g' \tau}\frac{\partial m}{\partial t'} = \frac{r^2}{\alpha'\tau}\frac{\partial m}{\partial t'} \qquad (41)$$

where $\alpha' = \rho_s k_g'/\rho$. The dimensionless group $\alpha'\tau/r^2$ corresponds to the Fourier number $\alpha t/r^2$, which appeared in the analytic solutions. Corresponding to the Biot number is the group $h_g r/k_g'$ which appears when the surface boundary condition is written in dimensionless form. However, as $h_g r/k_g' \longrightarrow \infty$, the solution of equation (41) in terms of $\bar{m} - m_e$ will be a function only of $(\alpha'\tau/r^2)t'$. For specimens of the same shape, the group $\alpha'\tau/r^2$ is constant. Hence, for a given value of α', τ must vary as r^2.

The relationship between τ and r when $h_g r/k_g \longrightarrow 0$ can be determined in the general case from equation (18). k_g may be variable within the specimen, but since moisture gradients approach zero as $h_g r/k_g \longrightarrow 0$, the moisture content m can be considered constant throughout the specimen or $\bar{m} = m$. These conditions would be approximated by a block of wood coated with a paint film with a high resistance to the passage of moisture. If A is the total surface area of the specimen and V its volume, equation (18) can be written as

$$\rho V \frac{dm}{dt} = -P_s A h_g (m - m_e) \tag{42}$$

The ratio V/A can be written as Br where B is the same dimensionless shape factor that appears in equation (40). Equation (42) can then be written as

$$\frac{d \log (m - m_e)}{dt} = -\frac{P_s h_g}{B \rho r} = -\frac{1}{\tau} \tag{43}$$

which is identical to equation (40).

Preliminary Drying Rate Measurements

Although the details of the experimental work will not be given in this paper, some of the preliminary results of drying experiments will be briefly summarized to show the relationship between τ and the specimen dimension r for several different materials. Figure 5 shows a dimensionless log-log plot of τ/τ_o and r/r_o in which τ is the timelag for a specimen temperature

Figure 5.--The relationship between the timelag interval τ and the specimen dimension r in which τ/τ_o is shown as a function of r/r_o on a log-log plot. τ_o was chosen as 1 hour for all specimens. r_o was taken as 0.0867 inch for the birch dowels and sawdust layers and as 0.125 inch for the square basswood rods.

of 80°F. and r is the radius or half thickness depending on the type of specimen. The values of τ_o and r_o were chosen so that the average position of the data on the chart would be approximately the same for the three different kinds of specimens. These were square basswood rods which ranged from 0.07 inch to 3.70 inches in diameter, round birch rods from 0.063 inch to 1.00 inch in diameter, and loosely packed sawdust layers 0.27 inch to 4.00

inches thick. The sawdust layers were in metal trays and could lose moisture from only one side, so the effective range of thickness was double the preceding range of values. The line through the data represents the theoretical second power scaling relationship between τ and r which should exist when $h_g r/k_g$ is large. With the exception of the points representing the smallest birch rod and the smallest basswood rod (and also the points for the two thinnest sawdust layers), the agreement of the data with the theoretical line is good. Possibly for the smaller specimens, $h_g r/k_g$ is small enough to cause deviation from the second power relationship between τ and r. It may be that solid woody materials with r less than 0.02 or 0.03 inches, or sawdust layers with r less than 0.1 inches, are in the region where τ varies as the first power of r. However, this has not yet been determined experimentally.

Figure 6 is an example of the drying curves, each of which yields one value for τ. In the basic curve, the quantity $\bar{m} - m_e$ is

Figure 6.--The quantity $\bar{m} - m_e$ for a square basswood rod 0.15 inch in diameter is plotted as a function of the drying time for a temperature of 80°F. and a relative vapor pressure of 0.41.

plotted as a function of the drying time t on a semi-log chart. With the exception of the first few measurements, the points tend to fall on a straight line, the slope of which determines the time-lag τ . The intersection of this line with the t = 0 ordinate gives the value of $\bar{m}_o - m_e$, which appears in equation (30).

The value of k_g for any given specimen can be estimated from the equation

$$k_g = \frac{r^2}{N_1^2} \frac{\rho}{\tau \rho_s}$$

Excluding the smallest specimen in each group, the mean values of k_g for the birch and basswood rods was 2.34×10^{-11} seconds and 3.12×10^{-11} seconds, respectively. For the sawdust layers the mean value of k_g was much greater, about 17.4×10^{-11} seconds with the thinnest layer excluded. Apparently vapor diffusion in the air spaces of the sawdust made it a much better conductor of moisture than solid wood substance. This effect should be present even in a greater degree in some types of forest fuels such as layers or beds of conifer needles.

The data for figure 6 were obtained by weighing the basswood specimens (six square rods 12 inches long and 0.15 inch in diameter) at about 10-minute intervals while they dried in a room of nearly

constant temperature and constant relative vapor pressure. At the end of the drying period, the rods were ovendried and the $\bar{m} - m_e$ values computed. The value of m_e was taken as 0.09 throughout the period.

Possible Effects of Air Movement, Radiation, and Evaporation Cooling

There are complex interactions between air movement, solar radiation, and evaporation cooling in their combined effect on the rate of drying of forest fuels. With the exception of the early stages of the drying period, evaporation cooling should have little effect on the drying rate if $h_g r/k_g$ is large. In the absence of radiation, wind should also have but little effect on the drying rate of solid material if $h_g r/k_g$ is large. Byram (12) showed that specimens in bright sunlight will have a lower drying rate if there is wind than if there is no wind. In this case, the convective cooling of an airstream partially offsets the temperature rise due to radiation and results in a smaller value of P_s. If $h_g r/k_g$ was very small, the combined effect of wind, sun, and evaporation would be determined by the product $h_g P_s$ in equation (43). Air movement would increase h_g and radiation would increase P_s. On the other hand evaporation cooling and convective cooling (in the presence of intense radiation) would tend to limit the increase of P_s.

Although the relationships have not been determined experimentally, air movement should have a greater effect on the drying of porous materials such as beds of conifer needles or hardwood leaves, than for solid material. The transport of water vapor out of the interior spaces by penetrating air currents should result in a marked increase in k_g.

CONCLUSION

Depending on the nature of the moisture flow problem, some choices of the gradient, or "driving force," which induces the moisture flow, are more suitable than others. However, in a mathematical sense there appears to be no preferred choice.

Analytic solutions to the moisture transfer equations, based on the assumption of constant properties, give approximate but useful descriptions of the drying process for a variety of forest fuel materials. In addition they result in a better insight to some complex features of moisture flow, such as those involving surface transfer phenomena. However, some of the most significant relationships, such as the first and second power scaling relationships between η and r, can also be deduced by other methods. These do not require the assumption of constant properties, nor do they require a solution of the differential equations. Either approach leads

to basic relationships which are helpful in understanding and predicting the interacting effects of wind, solar radiation, and evaporation cooling in the drying of forest fuels.

REFERENCES

(1) Byram, George M. Sun and wind and fuel moisture. Jour. Forestry (38): 639-640 (1940).

(2) Carslaw, H. S. and J. C. Jaeger. Conduction of heat in solids. Oxford Univ. Press, London (1959).

(3) Crank, J. The mathematics of diffusion. Oxford Univ. Press, London (1957).

(4) Eckert, E. R. and Robert M. Drake, Jr. Heat and mass transfer. McGraw-Hill Book Co., New York (1959).

(5) Giedt, W. H. Principles of engineering heat transfer. D. Van Nostrand Co., Princeton (1957).

(6) Hougen, O. A., H. J. McCauley, and W. R. Marshall. Limitations of diffusion equations in drying. Trans. Amer. Inst. Chem. Engrs. 36(2): 183-209 (1940).

(7) Marshall, W. R. and S. J. Friedman. The drying of solids. Chem. Engrs. Handbook, McGraw-Hill, New York: 800-884 (1950).

(8) Sherwood, T. K. The drying of solids-I. Indust. and Eng. Chem., 21(1): 12-16 (1929).

(9) Spalt, H. A. The sorption of water vapor by domestic and tropical wood. Tech. Rpt. No. 9, Properties of Tropical Woods, Yale Univ. School of Forestry (1957).

(10) Stamm, A. J. Passage of liquids, vapors, and dissolved materials through softwoods. U. S. Dept. Agr. Tech. Bul. 929 (1946).

(11) Tuttle, Fordyce. A mathematical theory of the drying of wood. Jour. Franklin Institute (200): 609-614 (1925).

(12) Van Arsdel, W. B. Approximate diffusion calculations for the falling-rate phase of drying. Trans. Amer. Inst. Chem. Engrs. 43(1): 13-24 (1947).

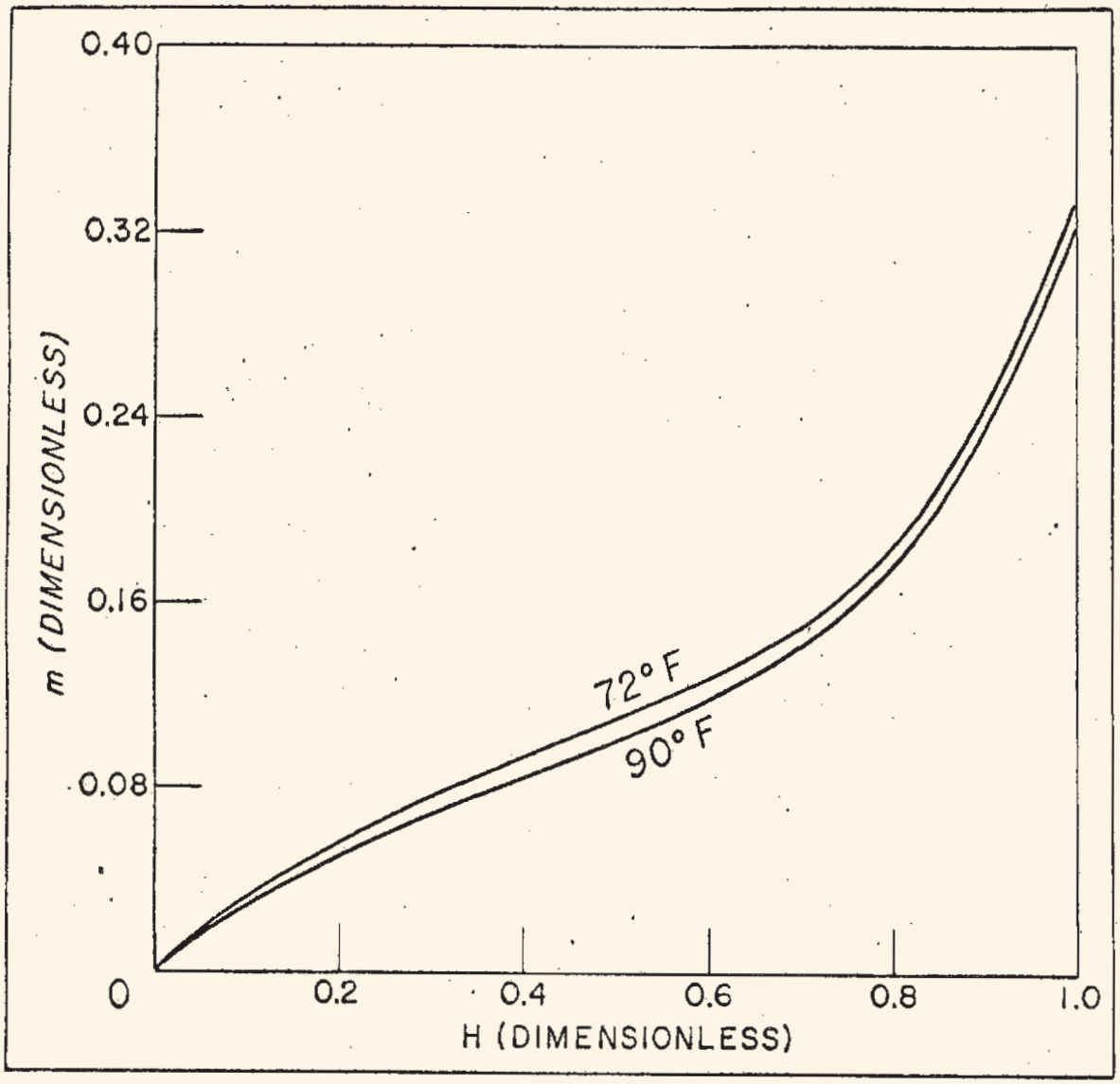

Figure 1.--Vapor pressure isotherms for temperatures of 72°F. and 90°F. show the moisture content m plotted as a function of the relative vapor pressure H. These curves are those which Spalt (9) obtained for basswood for desorption conditions.

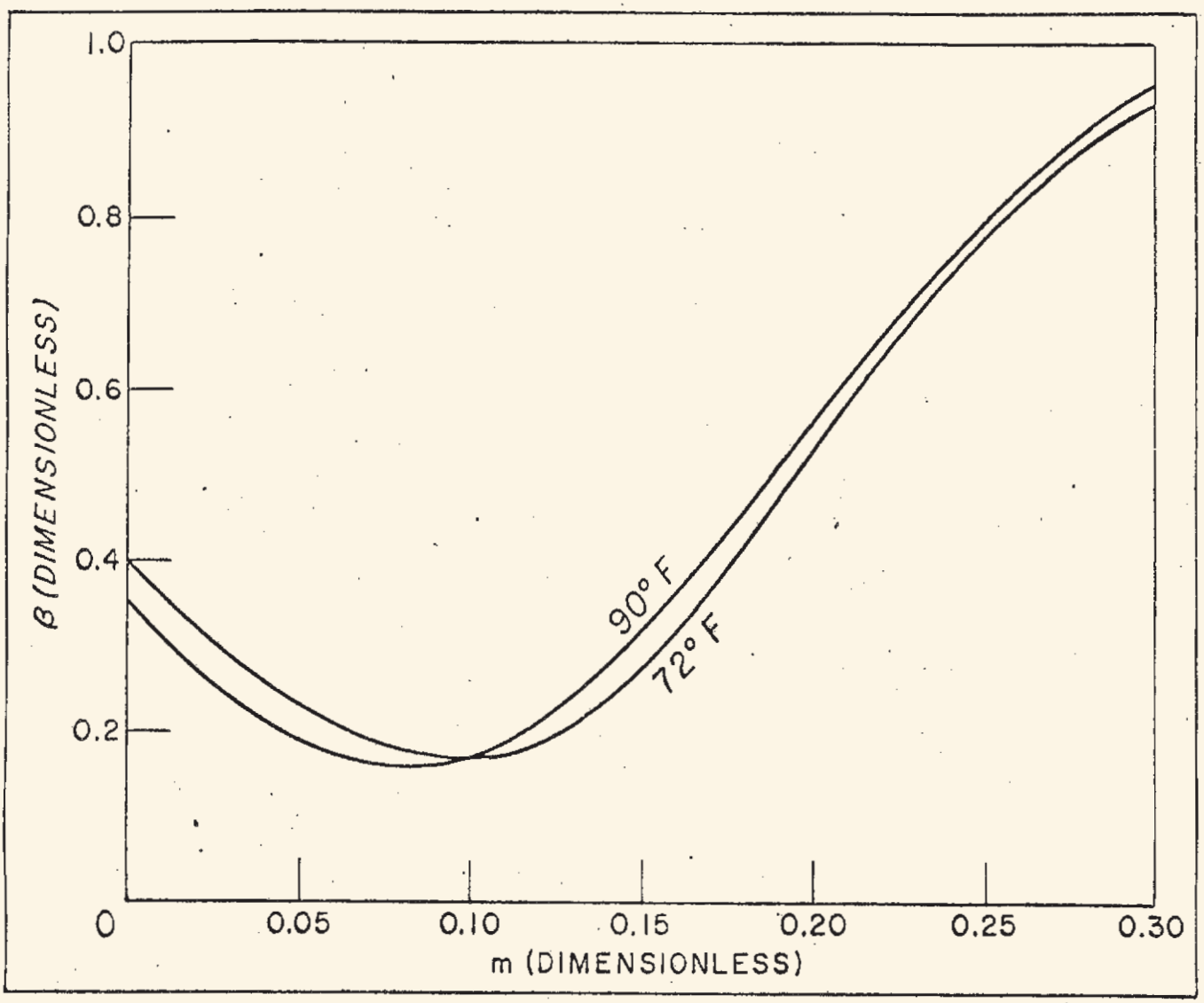

Figure 2.--The parameter β is shown as a function of the moisture content m for temperatures of 72°F. and 90°F. The ordinates of these curves are equal to the slopes of the curves in figure 1.

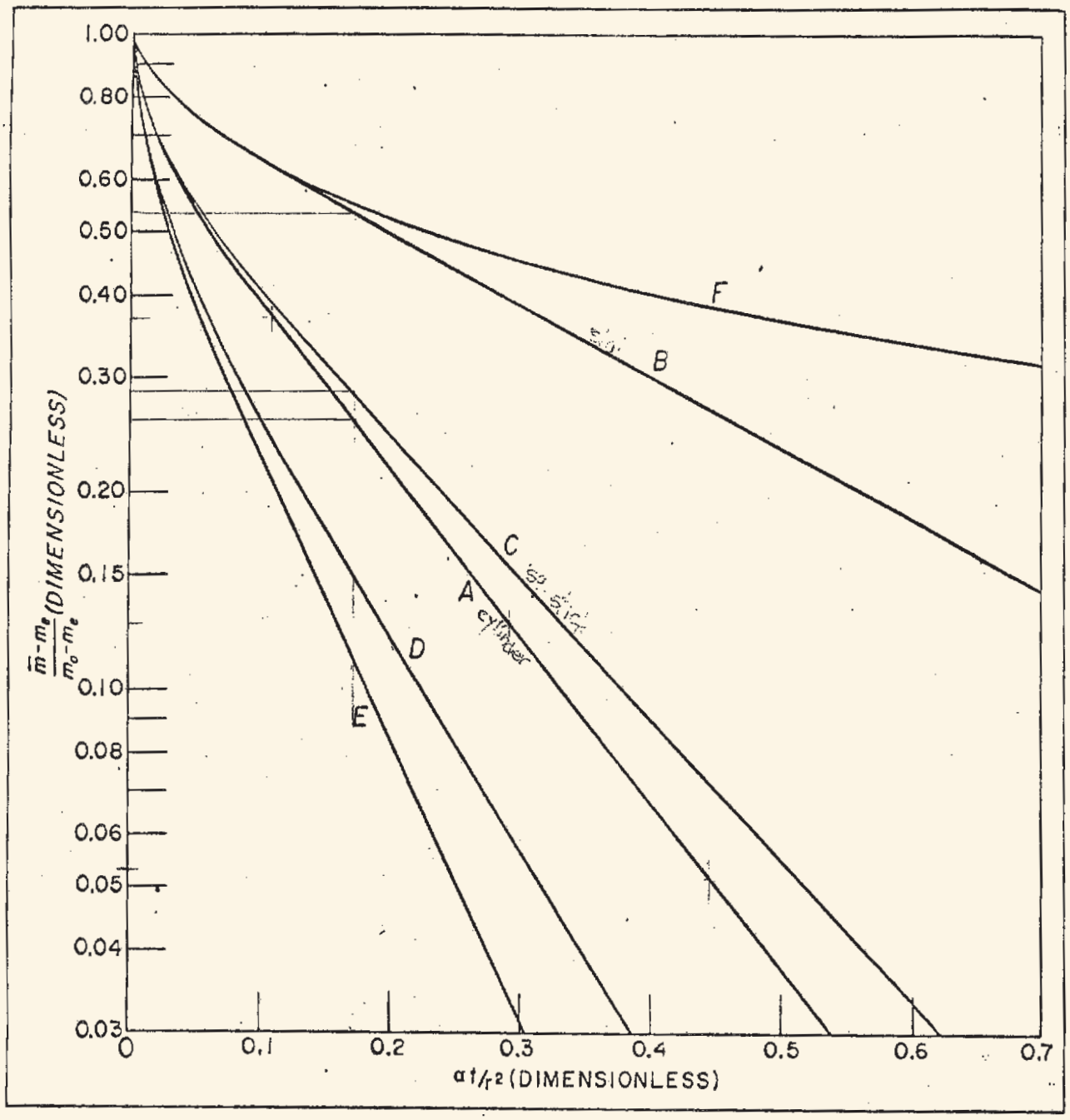

Figure 3.--Theoretical drying curves for specimens with six different geometric forms: A, cylinder; B, infinite plane slab; C, infinite square rod; D, cube; E, sphere; F, semi-infinite solid. The ratio $(\bar{m}-m_e)/(m_o-m_e)$ is plotted as a function of the Fourier number

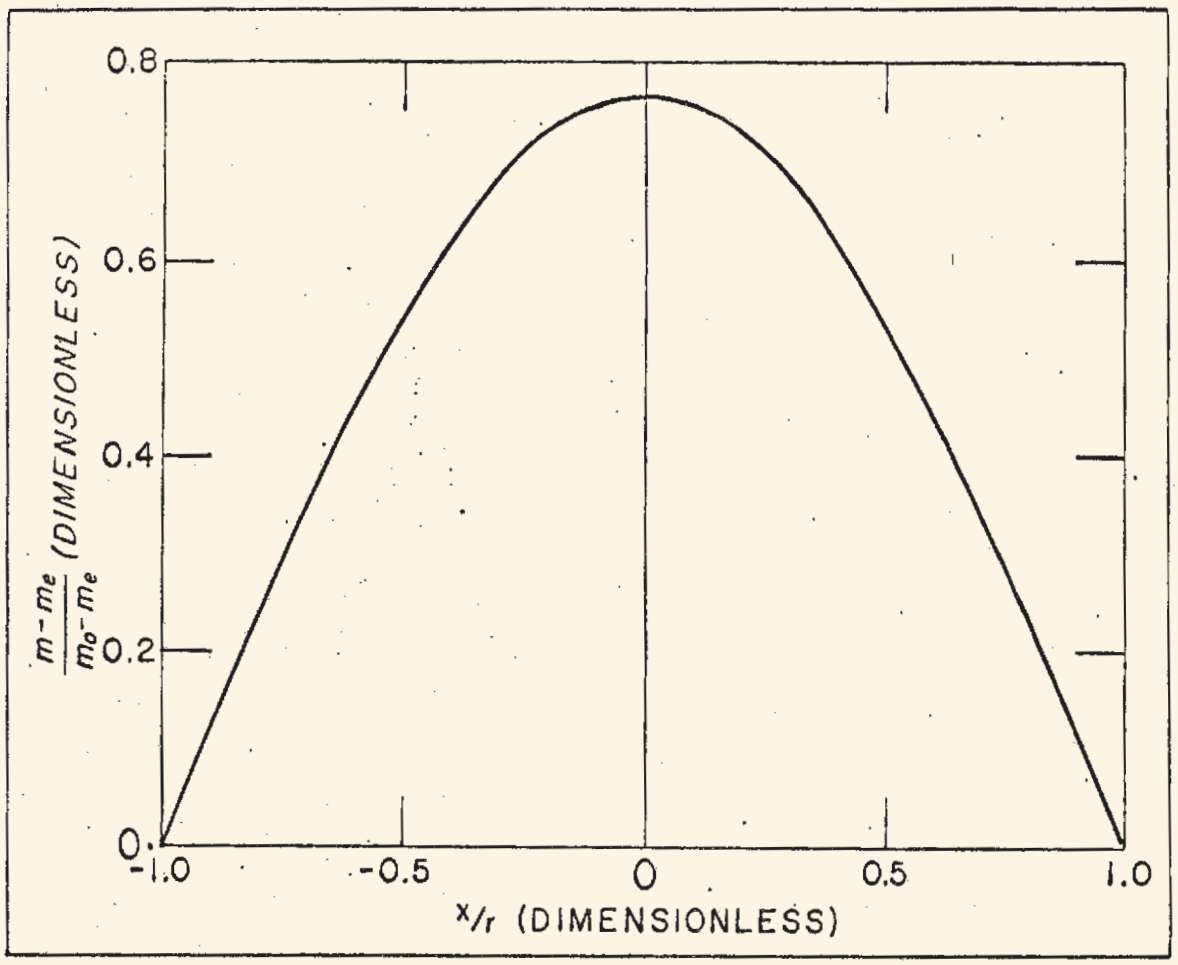

Figure 4.--The theoretical distribution of moisture across a plane slab at time t = $\tau/2$.

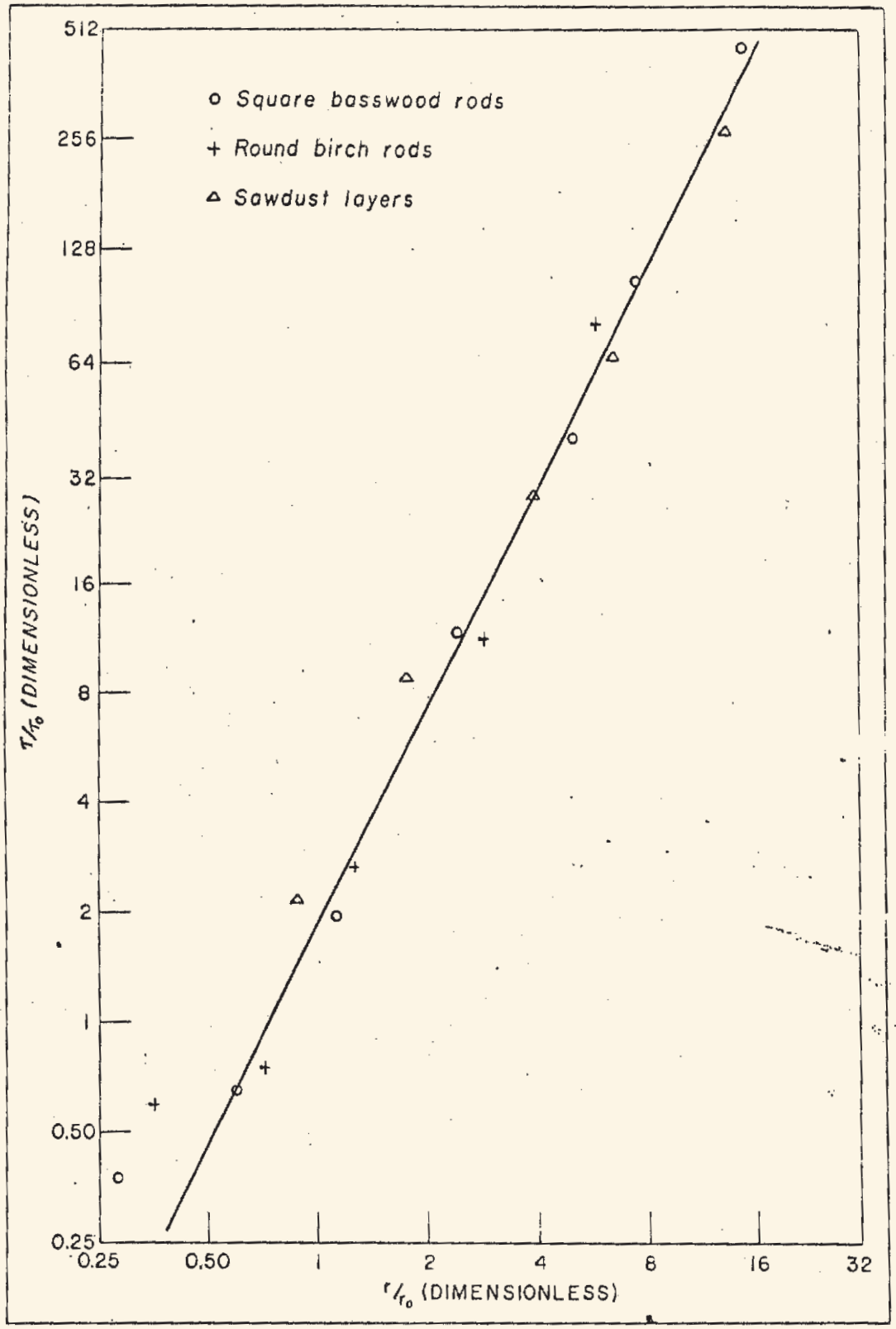

Figure 5.--The relationship between the timelag interval τ and the specimen dimension r in which τ/τ_o is shown as a function of r/r_o on a log-log plot. τ_o was chosen as 1 hour for all specimens. r_o was taken as 0.0867 inch for the birch dowels and sawdust layers

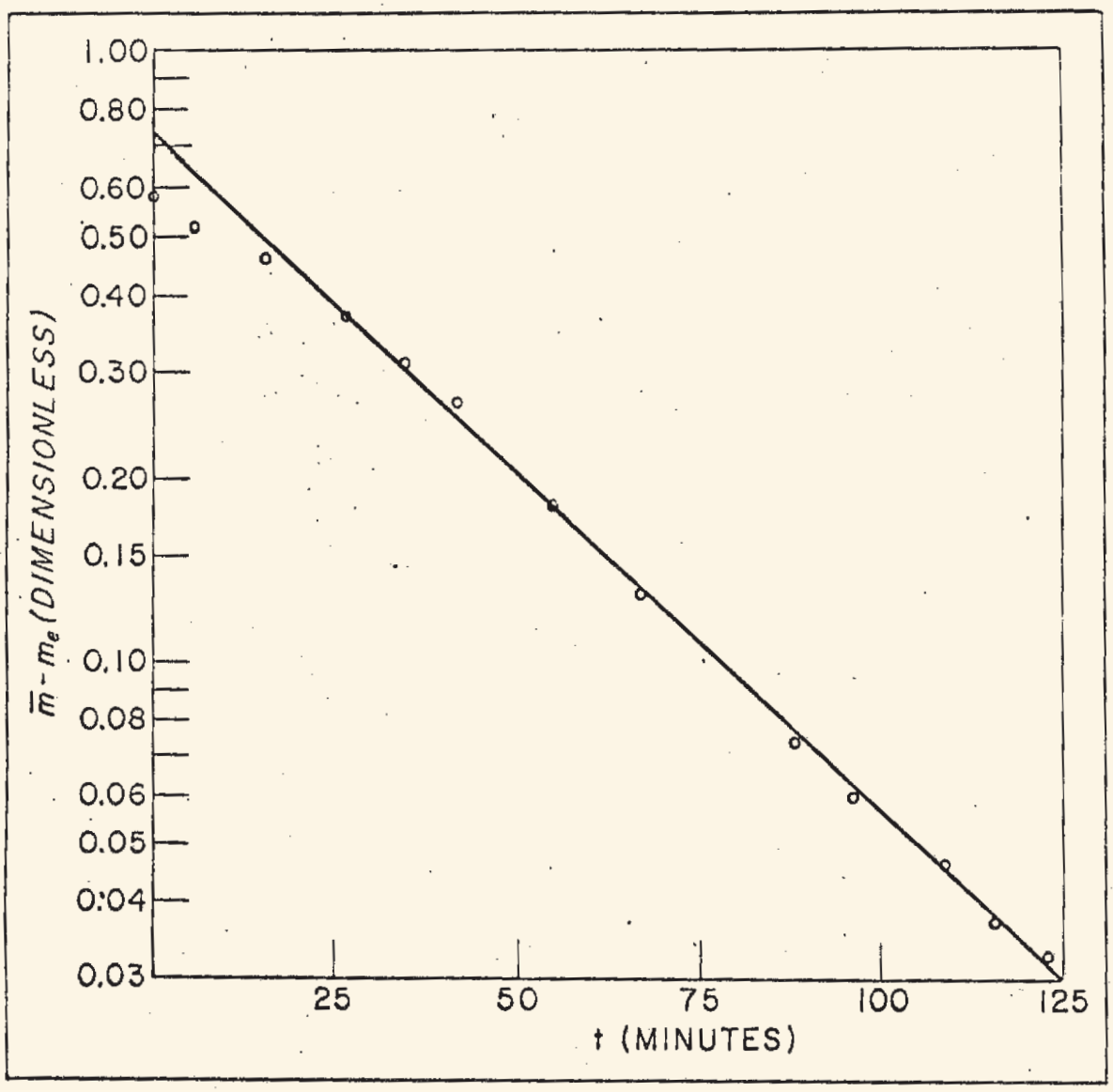

Figure 6.--The quantity $\bar{m} - m_e$ for a square basswood rod 0.15 inch in diameter is plotted as a function of the drying time for a temperature of 80°F. and a relative vapor pressure of 0.41.

Byram, G.M.; Nelson, R.M. 2015. An analysis of the drying process in forest fuel material. e-Gen. Tech. Rep. SRS-200. Asheville, NC: U.S. Department of Agriculture Forest Service, Southern Research Station. 45 p.

It is assumed that the flow of moisture in forest fuels and other woody materials is determined by the gradient of a quantity g which is a function of some property, or properties, of the moisture content. There appears to be no preferred choice for this function, hence moisture transfer equations can be based on a number of equally valid definitions of *g*. The physical meaning and dimensions of the mass conductivity k_g will depend on the definition of *g* but the mass diffusivity α is independent of *g*.

Simplified solutions to the transfer equations are expressed in terms of the ratio t/τ. The timelag τ is a measure of the drying rate. It scales as the second power of the appropriate dimension of the specimen, such as the half thickness, when the Biot number is large but scales as the first power of the characterizing dimension when the Biot number is small. Analytic solutions are not possible when properties are variable but the scaling relationships remain unchanged.

The basic theory of the drying process throws considerable light on the complex interacting effects of air movement, radiation, and evaporation cooling on the drying rates of forest fuel material.

Keywords: Down woody material, drying rates, fire, forest fuel moisture, fuel drying process, moisture transfer.

How do you rate this publication?

Scan this code to submit your feedback or go to www.srs.fs.usda.gov/pubeval